Article

Not peer-reviewed version

Zinc Nanoparticle Effects on the Green Leaf Volatiles and Phyllosphere Bacteriome in *Capsicum annum* Seedlings

García-Casillas Luis Alberto , Reyes-Maldonado Oscar Kevin , Sánchez-Fernández Rosa , Zúñiga Mayo Víctor , Zamudio-Ojeda Adalberto , Lomelí-Rosales Diego Alberto , Cortez-Álvarez César Ricardo , Rebeca Escutia Gutiérrez , Guevara-Martínez José Santiago , Velázquez-Juárez Gilberto *

Posted Date: 5 January 2026

doi: 10.20944/preprints202601.0199.v1

Keywords: *Capsicum annuum*; ZnO nanoparticles; green leaf volatiles (GLVs); methyl salicylate; phyllosphere; oxidative stress

Article

Zinc Nanoparticle Effects on the Green Leaf Volatiles and Phyllosphere Bacteriome in *Capsicum annum* Seedlings

García-Casillas Luis Alberto [1], Reyes-Maldonado Oscar Kevin [1], Sánchez-Fernández Rosa [2], Zúñiga Mayo Víctor [3], Zamudio-Ojeda Adalberto [4], Lomelí-Rosales Diego Alberto [1], Cortez-Álvarez César Ricardo [5], Rebeca Escutia Gutiérrez [5], Guevara-Martínez José Santiago [5] and Velázquez-Juárez Gilberto [1,*]

[1] Chemistry Department. Laboratory of Advanced Biochemistry. University of Guadalajara, Mexico
[2] Laboratorio Nacional de Investigación y Servicio Agroalimentario y Forestal (LANISAF), Universidad Autónoma Chapingo, Mexico
[3] Campus Montecillo, CONACyT-Instituto de Fitosanidad, Colegio de Postgraduado, Mexico
[4] Physics Department, University of Guadalajara, Mexico
[5] Pharmacology Department, University of Guadalajara, Mexico
* Correspondence: gilberto.velazquez@academicosu.udg.mx

Abstract

The use of zinc oxide nanoparticles (ZnONPs) in agriculture has increased due to their biostimulant potential; however, their effects on plant chemical communication and associated microbial communities are still poorly understood. This study presents a multi-perspective analysis contrasting the effects of ZnONPs with those of conventional ZnO (Bulk) on *Capsicum annuum* seedlings grown in a substrate with concentrations of 50 and 500 mg kg^{-1}. The results reveal that, at high doses, the bulk material (B500) generated a higher foliar accumulation of zinc (128.7 mg kg^{-1}) than ZnONPs (NP500, 119.7 mg kg^{-1}), a phenomenon attributed to the agglomeration of nanoparticles in the soil matrix, which limits their root absorption. At the physiological level, a critical divergence was observed: while bulk ZnO stimulated the activity of the enzyme superoxide dismutase (SOD), ZnONPs caused severe inhibition of the same (93% reduction), compromising the enzymatic antioxidant machinery and forcing the plant to rely on non-enzymatic mechanisms, such as an increase in total phenols. The volatilomic profile revealed a specific metabolic disturbance induced by ZnONPs in the green leaf volatiles (GLV) pathway. A significant accumulation of hexanal and suppression of hexanol and hexyl acetate were detected, suggesting that the nanomaterial inhibited alcohol dehydrogenase (ADH). In addition, ZnONPs suppressed the emission of methyl salicylate (MeSA)—a key messenger in acquired systemic resistance—whereas the Bulk treatment increased its abundance to 41.7%. Finally, metagenomic analysis indicated that zinc stress restructured the phyllosphere microbiota, promoting the proliferation of Actinobacteria and eliminating sensitive taxa such as Spirochaetes. Taken together, these findings demonstrate that ZnONPs act as multifactorial stressors that not only alter internal metabolism but also silence chemical communication and remodel plant ecology.

Keywords: *Capsicum annuum*; ZnO nanoparticles; green leaf volatiles (GLVs); methyl salicylate; phyllosphere; oxidative stress

1. Introduction

Plant cultivation is a cornerstone of food security, where improving crop yield is a key objective. To achieve this goal, different agricultural practices and technologies are employed, drawing upon

 doi:10.20944/preprints202601.0199.v1

multiple fields of knowledge; among them, nanotechnology, which has gained significant relevance in recent years due to its potential applications in agriculture [1]

Chili pepper is one of the most widely cultivated vegetables globally. In 2023, 38.31 million metric tons were produced, with an economic value of USD 34.92 billion, ranking it as the eighth-most-produced crop worldwide [2]. The fruits of the genus *Capsicum* are called chili peppers, five of which are domesticated and cultivated across regions: *C. baccatum*, *C. frutescens*, *C. pubescens*, *C. chinense*, and *C. annuum* [3,4]. This vegetable is consumed both fresh and dried; it serves as a key raw material in the cosmetics and food industries and is an essential component of traditional dishes in numerous countries. Chili peppers are rich sources of vitamins C and E, flavonoids, and carotenoids. Additionally, they produce capsaicinoids, bioactive compounds with analgesic, anti-carcinogenic, and antimicrobial properties [5,6]. However, the productivity of this solanaceous crop is often limited by biotic and abiotic stresses, which has catalyzed the search for more efficient biofortification and crop protection strategies.

Nanotechnology has emerged as a disruptive tool in plant physiology, with the potential to enable precision agriculture through nanofertilizers and nanolecitors. Among these, zinc oxide nanoparticles (ZnONPs) have attracted particular attention. Zinc is an essential micronutrient that serves as a catalytic or structural cofactor for more than 300 enzymes, including superoxide dismutase (Cu/Zn-SOD) and alcohol dehydrogenase, thereby regulating vital processes ranging from protein synthesis to cell membrane integrity and antioxidant defense [7]. While numerous studies have documented that ZnONPs can enhance germination and growth in *Capsicum* by modulating nitrogen metabolism and hormonal activity [8], the boundary between biostimulation and phytotoxicity is thin and intrinsically dependent on particle size, concentration, and route of exposure. For example, studies have reported beneficial effects of ZnONP application on various crops, including chili pepper [1,9,10]. Several studies indicate that concentrations of ZnONPs ranging from 50 to 1000 ppm positively influence germination rates and seedling biomass in chili pepper plants [11–15].

Furthermore, ZnONPs have demonstrated efficacy in mitigating biotic stress by inhibiting the growth of fungal pathogens such as *Fusarium oxysporum* and *Colletotrichum capsici*, exhibiting nematicidal activity against *Meloidogyne incognita* [16,17], and reducing disease severity caused by the Pepper Huasteco Yellow Vein Virus [18]. ZnONPs also enhance chili plants' tolerance to abiotic stresses. Exogenous application of 1000 ppm ZnONPs improves salinity stress tolerance by stimulating the plant's antioxidant defense system [19]. Moreover, both *in vitro* and pot experiments have shown that ZnONPs increase chili plant biomass and mitigate the negative impact of cadmium stress on chlorophyll accumulation [20,21]. However, assessments of the effects of nanomaterials have focused on physiological parameters such as biomass, chlorophyll content, and antioxidant enzymes, overlooking other metabolic aspects of plants, including the profile of Volatile Organic Compounds (VOCs), specifically Green Leaf Volatiles (GLVs). GLVs, which comprise aldehydes, alcohols, and six-carbon (C6) esters, are rapidly synthesized via the lipoxygenase (LOX) and hydroperoxide lyase (HPL) pathways in response to mechanical damage or stress [22]. Far from being mere metabolic byproducts, GLVs constitute a sophisticated chemical "language" that allows the plant to activate direct and indirect defenses, and to alert neighboring plants to imminent threats (priming phenomenon) [23,24]. Interference by ZnONPs in key enzymes in this pathway, such as lipoxygenase or alcohol dehydrogenase, could silence or alter these vital signals, with unknown ecological consequences [25]. At the same time, the surface of plants (phyllosphere), represents one of the most extensive and hostile microbial habitats on the planet, colonized by a diverse community of bacteria known as the phyllosphere bacteriome [26]. These microorganisms form a biotic barrier that protects against pathogens, fixes atmospheric nitrogen, and modulates host physiology through the production of phytohormones [27]. Given that ZnONPs possess intrinsic antimicrobial properties, capable of inducing oxidative stress and membrane disruption in prokaryotic cells [28], their accumulation in leaf tissues following root absorption and translocation could exert drastic selective pressure on this ecosystem.

 doi:10.20944/preprints202601.0199.v1

This study proposes a multi-perspective analysis to elucidate the effects of ZnONPs on *Capsicum annuum*, contrasting them with conventional zinc oxide (Bulk ZnO). We investigate not only bioaccumulation and the classic enzymatic antioxidant response but also the volatilomic profile (GLVs and methyl salicylate) and the structure of the phyllosphere bacterial community. Our objective is to determine whether the nanometric scale induces metabolic and ecological changes different from the ionic or macrometric form, integrating the results to gain a better understanding of the subtle processes within plants.

2. Materials and Methods

2.1. Nanoparticle Characterization

Zinc oxide nanoparticles (ZnONPs) were synthesized in-house (Nanomaterials Synthesis Laboratory, CUCEI). The morphology and size of the ZnONPs were determined by transmission electron microscopy (TEM) using a JEOL 1010 instrument (JEOL, Tokyo, Japan) operated at an acceleration voltage of 80 kV and a magnification of 120,000X.

2.2. Experimental Design and Growth Conditions

The experiment was conducted using a completely randomized design. Seeds of *Capsicum annuum* var. Jalapeño M. (Caloro®, Jalisco, Mexico) were sown in a substrate mixture of agricultural soil and perlite (1:1, v/v). The treatments consisted of a negative control without ZnO (Ctrl) and four treatments with ZnO: two with nanoparticles at 50 and 500 mg kg^{-1} dry substrate (NP50 and NP500) and two with bulk (macrometric) ZnO at the same concentrations (B50 and B500). Thirty replicates were established for each treatment. For substrate preparation, the required mass of each ZnO form was manually homogenized into 10 kg of dry substrate for 20 min. The mixture was then distributed into 250 mL plastic pots. Three seeds were sown per pot at a 2 mm depth. Pots were kept in darkness at 27°C for 7 days to promote germination and subsequently transferred to a greenhouse at the Colegio de Postgraduados, Campus Montecillo, Mexico (19°27'40" N, 98°54'13" W). Plants were grown for 42 days (June 7 to July 19, 2024). Every three days, each pot was irrigated with 70 mL of a nutrient solution containing 120 ppm N, 24 ppm P, and 155.2 ppm K.

2.3. Sample Processing and Preservation

At 42 days post-sowing, fresh leaf tissue from 45 seedlings per treatment was collected for metabolomic and metagenomic analyses. From the remaining seedlings, true leaves and cotyledons were collected, pooled to form a composite sample per treatment, immediately frozen in liquid nitrogen, and lyophilized in a FreeZone 4.5 freeze-dryer (LABCONCO®, Kansas City, MO, USA) at -52°C and 0.052 mBar for 72 h. The dried tissue was pulverized and stored at -80°C.

2.4. Zinc Quantification in Plant Tissues

Zinc content was determined by atomic absorption spectroscopy (AAS). A 200 mg aliquot of lyophilized tissue was subjected to acid digestion with 3 mL of 65% nitric acid and 3 mL of 70% perchloric acid at 300°C for 40 min. The digest was diluted to 25 mL with 2% (v/v) nitric acid and filtered through a 0.45 µm nylon syringe filter. Zinc concentration was measured using a SpectraAAS 220 FS spectrophotometer (Varian, Palo Alto, CA, USA) at a wavelength of 213.9 nm. Quantification was performed against a standard curve prepared from a 100 mg L^{-1} stock solution, with concentrations ranging from 0 to 2.0 mg L^{-1}. Results were expressed as mg Zn per kg of dry weight (mg kg^{-1} DW).

2.5. Non-Enzymatic Antioxidant Activity and Total Polyphenols

Methanolic extracts were prepared by macerating 20 mg of lyophilized tissue in 10 mL of 80% (v/v) methanol for 24 h with orbital shaking in darkness. The mixture was centrifuged at 4,500 rpm

 doi:10.20944/preprints202601.0199.v1

for 10 min, and the supernatant was collected and stored at -20°C. All absorbance measurements were performed on a Multiskan SkyHigh microplate spectrophotometer (Thermo Fisher Scientific®, Waltham, MA, USA).

2.5.1. ABTS Assay

Radical scavenging activity was determined following the method of Stratil et al. [29]. The assay was performed at 734 nm, and results were expressed as mmol Trolox equivalents per gram of dry weight (mmol TE g^{-1} DW). Colocar que la molécula de referencia en los tres casos fue TROLOX.

2.5.2. DPPH Assay

Free radical scavenging activity was measured according to Brand-Williams et al. [30]. Absorbance was read at 515 nm, and results were expressed as mmol TE g^{-1} DW.

2.5.3. FRAP Assay

Ferric reducing antioxidant power was assayed as described by Benzie and Strain [31]. Absorbance was measured at 593 nm, and results were expressed as mmol TE g^{-1} DW.

2.5.4. Total Polyphenol Content

Total polyphenols were quantified using the Folin-Ciocalteu method [32]. Gallic acid was used as the standard. Absorbance was measured at 750 nm after 2 h of incubation. Results were expressed as mg gallic acid equivalents per gram of dry weight (mg GAE g^{-1} DW).

2.6. Antioxidant Enzyme Activity

Enzyme extracts were prepared by homogenizing 20 mg of lyophilized tissue in 2 mL of an ice-cold extraction buffer [0.1 M potassium phosphate (pH 7.5), 0.5 mM EDTA, 2% (w/v) PVP, and 0.5% (v/v) Triton X-100] using an ultrasonic bath for 10 min. The homogenate was centrifuged at 14,000 rpm for 10 min, and the supernatant was stored at -80°C.

2.6.1. Protein Quantification

Total protein content was determined using the Pierce™ BCA Protein Assay Kit (Thermo Fisher Scientific®) with bovine serum albumin (BSA) as the standard. Absorbance was read at 562 nm.

2.6.2. Guaiacol Peroxidase (GPOX)

GPOX (EC 1.11.1.7) activity was assayed by monitoring the formation of tetra-guaiacol at 470 nm, following the method of Castillo et al. [33].

2.6.3. Ascorbate Peroxidase (APX)

APX (EC 1.11.1.11) activity was determined by monitoring the decrease in ascorbate at 290 nm, as described by Nakano and Asada [34].

2.6.4. Catalase (CAT)

CAT (EC 1.11.1.6) activity was measured using the Catalase Colorimetric Activity Kit (Thermo Fisher Scientific®) according to the manufacturer's instructions. Absorbance was read at 560 nm.

2.6.5. Superoxide Dismutase (SOD)

SOD (EC 1.15.1.1) activity was determined by its ability to inhibit the photochemical reduction of nitroblue tetrazolium (NBT) at 560 nm, following Dhindsa et al. [35]. One unit of SOD activity was defined as the amount of enzyme required to cause 50% inhibition of NBT reduction.

 doi:10.20944/preprints202601.0199.v1

All enzyme activities were normalized by protein content and expressed in their respective units per mg of protein.

2.7. Volatile Organic Compound (VOC) Analysis

VOCs from fresh leaf tissue (1 g) were analyzed by solid-phase microextraction (SPME) coupled with gas chromatography-mass spectrometry (GC-MS). Samples were placed in 40 mL vials with 20 mL of 0.4% (w/v) NaCl solution and heated to 60°C. VOCs were extracted for 30 min using a DVB/CWR/PDMS fiber (Supelco®, Bellefonte, PA, USA) and desorbed for 15 min in the injection port of an Agilent 7890B GC system. Compounds were separated on an HP-5ms Ultra Inert column (30 m × 250 µm × 0.25 µm) and detected with an Agilent 5977A MSD. Tentative identification was performed by comparison against the NIST 14 spectral database, and conclusive identification was confirmed by comparing calculated Kovats retention indices (KRI) with values reported in the NIST Chemistry Web Book.

The analysis of volatile organic compounds (VOCs) was performed in 40 mL capacity solid phase microextraction (SPME) vials with polypropylene perforated lids and silicon/PTFE-coated septa, where 1 ± 0.005 g of fresh true leaves of 6 C. annuum L. seedlings were weighed for each of the treatments. Subsequently, 20 mL of 0.4 % (w/v) NaCl solution was added along with a magnetic bar and the joints of the vials were sealed, and subjected to shaking and heating at 60°C. Immediately afterwards, the VOCs present in this gas phase were extracted using a DVB/CWR/PDMS (Divinylbenzene/Carbon-WR/Polydimethylsiloxane) fiber with length of 10 mm and thickness of 80 µm (50/30 µm) (Supelco® , Bellefonte, PA, USA) with an exposure time of 30 min (Figure 2). Prior to use, the fiber was conditioned for 30 min at 260°C.

After exposure to VOCs, the fiber was manually inserted into injection port of an Agilent 7890B gas chromatograph (GC) (Agilent Technologies Inc., Santa Clara, CA, USA), operating in splitless mode at 240°C. The desorption time was 15 min, and the compounds were separated on an HP-5ms Ultra Inert capillary column (30 m x 250 µm x 0.25 µm) (Agilent Technologies Inc., Santa Clara, CA, USA) using the following chromatograph oven temperature program: 40°C for 3 min; heating to 280 °C at a rate of 10 °C/min; 280 °C for 2 min. The carrier gas was ultrapure Helium at a flow rate of 1 mL/min.

The chromatograph was coupled to an Agilent 5977A mass selective detector (MSD) (Agilent Technologies Inc., Santa Clara, CA, USA). The electron ionization energy was 70 eV, and the scanned mass range was 30 to 550 amu, with a scan rate of 13.8 spectra per second. The transfer line and ionization chamber temperatures were 250°C and 200°C, respectively. Data acquisition and processing were performed with the MassHunter Qualitative Analysis software system version 6.0 (Agilent Technologies, Inc., Santa Clara, CA, USA).

For the analysis of VOC production of *C. annuum*, two biological replicates were performed for each of the treatments. In addition, a blank was performed with an unsampled vial at the same conditions and a saline blank, and the compounds identified in these were removed from the data analyses.

VOCs from *Capsicum annuum* were tentatively identified based on their MS fragmentation patterns, compared with the National Institute of Standards and Technology (NIST) spectral database version 14.

Conclusive identification was carried out by comparing the Kovats retention index (KRI), calculated relative to the retention times of a series of n-alkanes (C7-C40), with the aid of the calculator developed by Lucero et al. [36], with the KRIs reported on an equivalent column and under the same analytical conditions in the NIST Chemistry Web Book (version 39).

Since the objective was not the determination of absolute amounts of each compound, the relative amounts of the individual compounds in each treatment were determined under the experimental conditions employed. The relative amounts were expressed as percentages of the peak area with respect to the total area of the chromatogram and as an average between the two replicates per treatment.

 doi:10.20944/preprints202601.0199.v1

2.8. Phyllosphere Microbiome Analysis

Total genomic DNA was extracted from 200 mg of fresh, composite tissue samples (hypocotyl, cotyledons, true leaves, apical bud) using the DNeasy PowerSoil Pro Kit (QIAGEN Inc., Aarhus, Denmark), following the manufacturer's protocol. The V1-V9 hypervariable regions of the 16S rRNA gene were amplified by PCR using primers 27F and 1492R with Ultra DNA Polymerase (Jena Bioscience GmbH, Jena, Germany). The amplicons were purified using the PCR Purification Kit (Jena Bioscience GmbH).

The purified amplicons were sequenced at Secoya Labs S.C. (Mexico City, Mexico) using Oxford Nanopore Technology on an R.10.4.1 flow cell. Basecalling was performed with Dorado (v. 7.3.9), and bioinformatic analysis was conducted with a minimum Q score of 10 and a minimum read length of 200 bp.

3. Results

3.1. Material Characterization

Both materials, ZnONPs and ZnO in bulk form, were characterized using scanning electron microscopy (SEM). Figure 1 shows three of the resulting micrographs. Figure 1a shows ZnO in bulk form, which has a significantly larger particle size than ZnONPs (Figure 1b). Similarly, enlarging the ZnONPs (Figure 1c) reveals that the nanoparticles predominantly have a rectangular morphology. Overall analysis of the sizes determined that the ZnONPs range in size from 20 to 120 nm, with an average size of 55 nm. 1 μm

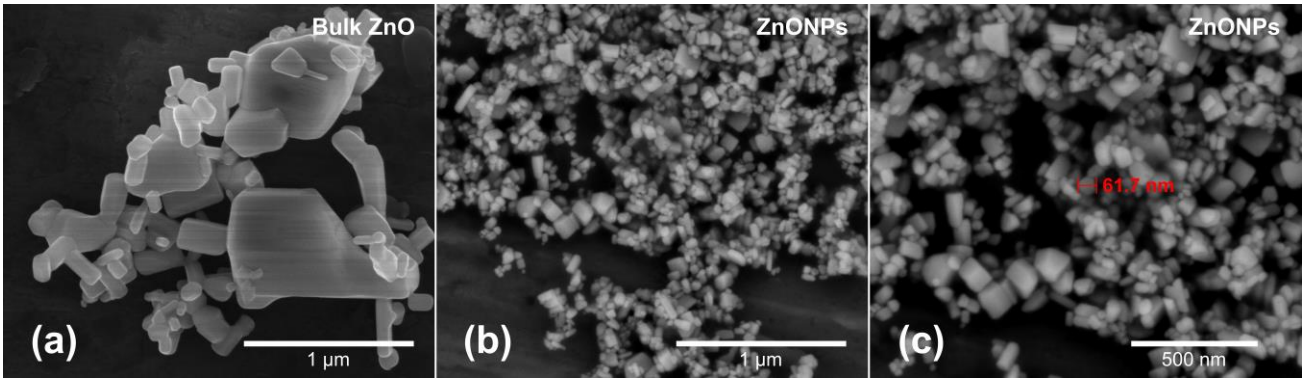

Figure 1. Comparative micrographs of bulk and nanoparticle ZnO materials. (a) Bulk ZnO, see the marked scale of 1 μm. (b) ZnONPs on the same scale of 1 μm. (c) Magnification of the field for nanoparticles, and representative measurement (in red) of the average particle size.

3.2. Bioaccumulation

We determined the total Zn concentration in seedling leaves utilizing atomic absorption spectroscopy (AAS). We found that all treatments (bulk and NPs) exhibited statistically significant differences in Zn concentrations compared to the control, as confirmed by Tukey's post hoc test ($p < 0.05$). Notably, the NP50 and B50 treatments showed an 8-9 % increase in Zn concentration, while the NP500 and B500 treatments demonstrated a substantial 35% and 45% increase, respectively. Table 1 presents the Zn concentrations for each treatment. Furthermore, the NP500 and B500 treatments showed a statistically significant difference with $p>0.05$, in our experiment, the amount of assimilated zinc and bioaccumulation factor was dose-dependent, but the efficiency of Zn accumulation was only dependent on the source (ZnONP or bulk) only if the concentration supplemented was high (500 mg kg^{-1}).

 doi:10.20944/preprints202601.0199.v1

Table 1. Zn content on freeze-drive leaves from seedlings treated. Treatments were either bulk ZnO (B50 and B500) or ZnNPs (NP50 or NP500).

Treatment	[Zn], mg kg^{-1}
Ctrl	88.55 ± 3.47 ^{a}
NP50	96.60 ± 2.98 ^{b}
B50	95.92 ± 2.51 ^{b}
NP500	119.7 ± 4.00 ^{c}
B500	128.7 ± 3.15 ^{d}

[1] Values are expressed as mg kg^{-1} of dry weight. [Zn] ± SD, n = 7. Different letters indicate statistically significant differences between treatments ($p < 0.05$) according to Tukey's post hoc test.

Several studies have examined Zn bioaccumulation in plants following the application of bulk Zn and ZnONPs. Zhang et al. [37] found that Zn assimilation was greater in the roots of *Schoenoplectus tabernaemontani* when exposed to ZnONPs than to Zn ions. In contrast, Cruz et al. [38] reported that in *Phaseolus vulgaris (L.) plants* exposed to ZnONPs and $ZnSO_4$, Zn bioaccumulation is more efficient when the particle size of ZnONPs is small (40 vs 300 nm). Our results are in agreement of Hoon et al. [39], where they studied the Zn content in leaves of *Brassica chinense* after the exposition to ZnONPs and $Zn(NO_3)_2$. They found that when a concentration of 100 mg kg^{-1} of both sources of Zn was used, no significant differences were detected, but if they used 500 or 1000 mg kg^{-1} of Zn, the accumulation of this metal increased when $Zn(NO_3)_2$ source was used instead of ZnONPs. It is worth mentioning that this effect was only seen when the nanoparticles used were larger than 30 nm in size.

3.3. Bacterial Community of the Capsicum annuum Phyllosphere

Several studies show that ZnONPs have an essential effect on the rhizosphere microbial community when applied to plants [40–42]. However, the impact of these nanoparticles has been little studied in the phyllosphere. We analyzed the phyllosphere bacterial community of chili plants treated with 50 and 500 mg/kg of soil using nanopore sequencing technology. From the sequencing data, microbial abundance and alpha diversity were calculated using the Shannon, Simpson, and Berger-Parker indices (Table 2). The Shannon and Simpson indices are similar in all samples, suggesting that ZnOPN has a slight impact on the abundance and diversity of the chili phyllosphere. The Berger-Parker index shows that the most abundant species in each sample comprises between 9.7 and 11% of the total, indicating that no single species dominates. In addition, bacterial species that are shared between the different treatments were analyzed, a species was considered present if it had in total ≥10 reads, after this cutoff 937 species were identified, of which 715 were present in all samples. In general, the Venn diagrams show that a low concentration of ZnO has little or no effect on the phyllosphere bacterial community, while a high concentration of ZnO (500 mg/kg) has an impact on the number of species, even though it was supplied in the soil. However, the effect does not depend on particle size (nano or bulk); moreover, most of the differences between Control vs NP500 and Control vs B500 are shared between NP500 vs B500 (Figure 2).

Table 2. Alpha-diversity indices of the phyllosphere microbiome across treatments.

Treatment	Shannon diversity index	Simpson's index	Berger-Parker index
Ctrl	4.11	0.960	0.100
NP50	4.16	0.960	0.100
B50	4.05	0.960	0.110
NP500	4.23	0.963	0.097
B500	4.30	0.960	0.100

 doi:10.20944/preprints202601.0199.v1

At the phylum level, Proteobacteria did not show changes in the different treatments, while in Spirochaetes the different ZnO treatments caused a decrease in the relative abundance of the species, where B50 presented the greatest effect. In the case of Cyanobacteria, a slight increase in the relative abundance of the species was observed at low concentrations of ZnO, while in Synergistetes and Bacteriota this same behavior was observed but at high concentrations of ZnO. This increase in the relative abundance of the species was greater in the Firmicutes, especially in the B500 condition. The greatest effect of the application of high concentrations of ZnO was observed in the Actinobacteria, since in that phylum the relative abundance of the species increases considerably. In addition, these high concentrations seem to favor the colonization of species from the Gemmatimonadetes (Figure 3).

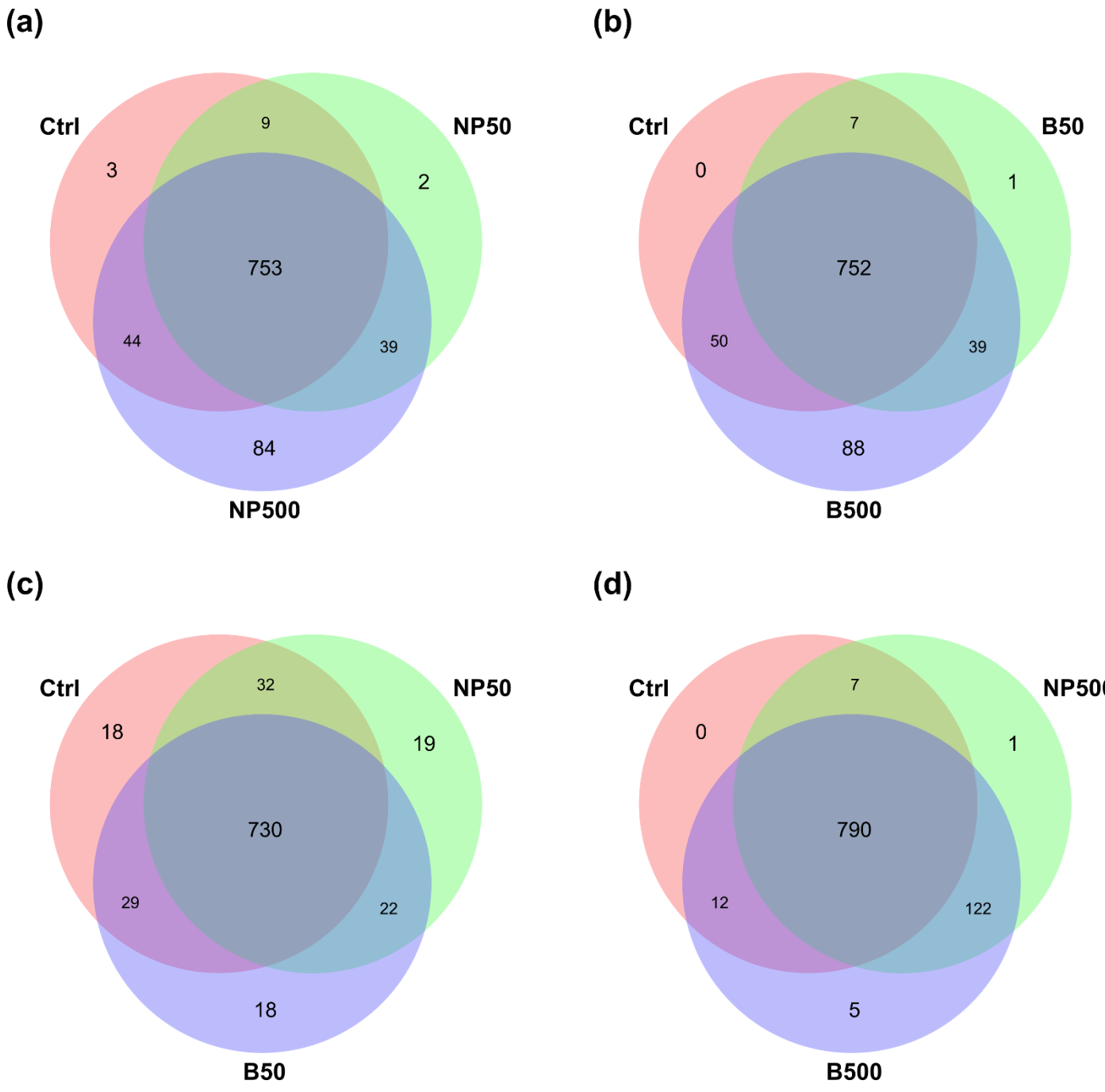

Figure 2. Venn diagrams of the number of shared species among treatments.

 doi:10.20944/preprints202601.0199.v1

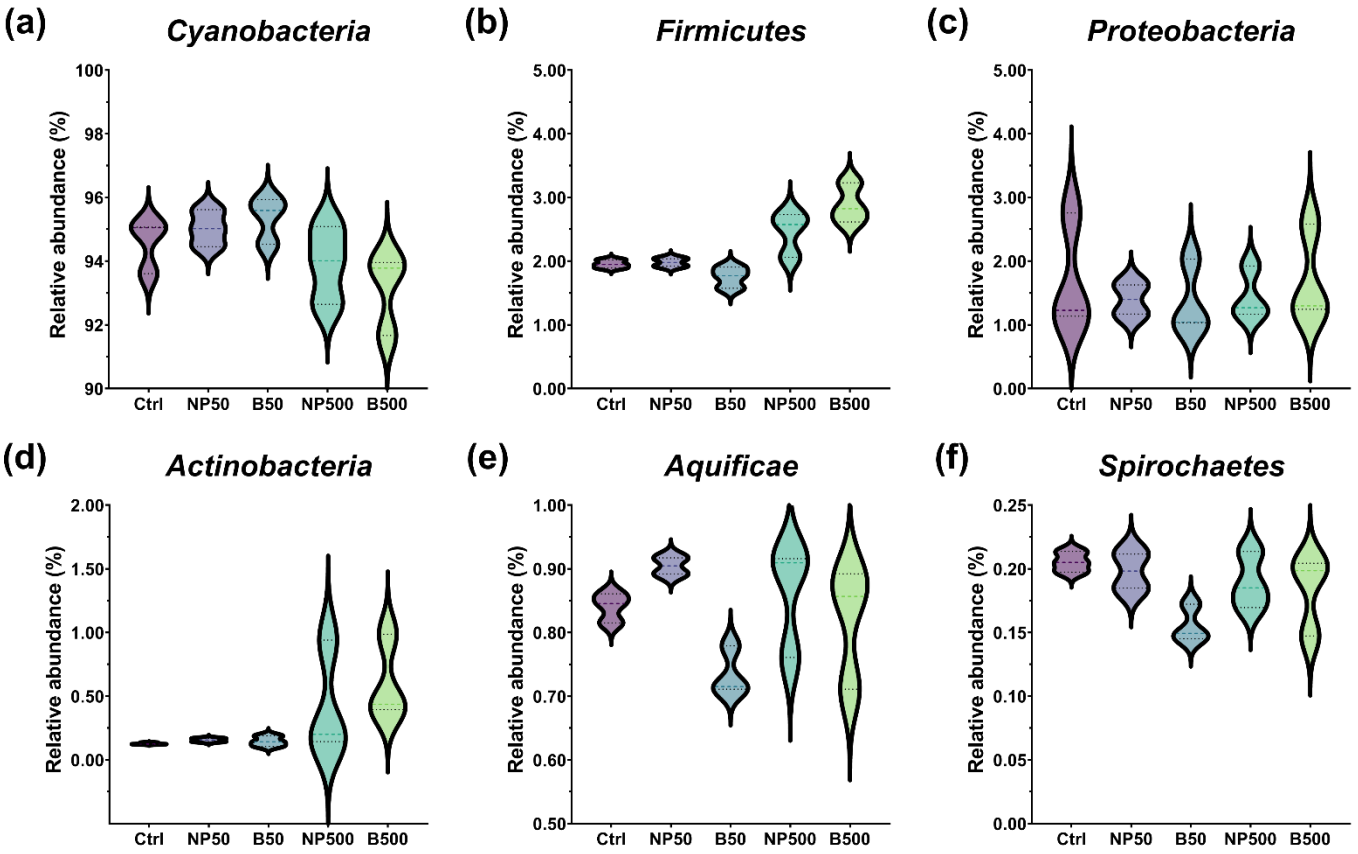

Figure 3. Violin plots showing the variation in relative abundance of the most representative bacterial phyla across treatments.

3.4. Metabolic Activities

3.4.1. Antioxidants

The antioxidant capacity of the different treatments was determined by three different techniques: ABTS, DPPH, and FRAP (Figure 4A-C.) The values of each analysis correspond to an extract of 2 mg/ml for each treatment. Trolox was used as a reference antioxidant in all cases, and results were expressed as mmol Trolox/g dry weight to facilitate comparison of results across methods. For TPC determination (Figure 4D), gallic acid was used as a reference, and the results were expressed as gallic acid equivalents (mg) per g dry sample.

Antioxidant activity results show statistically significant differences among treatment samples compared to the control group, as confirmed by Tukey's post hoc test ($p < 0.05$). A similar pattern was observed across all cases: an increase in antioxidant capacity in treatments with ZnONP or the bulk form compared with the control group. Using the DPPH assay as a reference, an increase of 20-22% was observed in all treatments, except for treatment B500, where the increase was much higher, reaching 50%.

Regarding the total phenolic compound content (TPC), an increase of 13-16% was observed in all treatments compared to the control group, except for NP500, where no statistically significant differences were found. Compared with results obtained using the various techniques employed to assess antioxidant capacity, a downward trend was observed for NP500 and B500. This suggests that, in these cases, the antioxidant activity does not depend exclusively on phenolic compounds but also involves other molecules of a different chemical nature.

 doi:10.20944/preprints202601.0199.v1

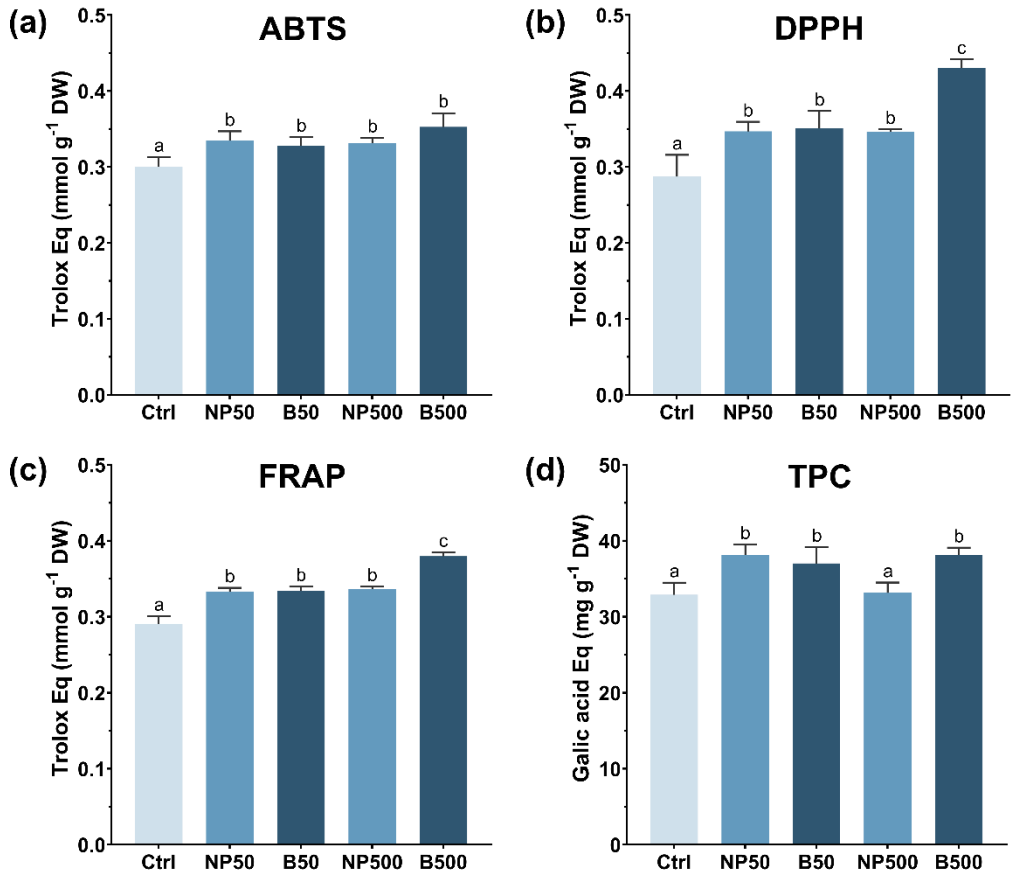

Figure 4. Effect of the application of nano (NP) and bulk (B) ZnO on antioxidant capacity evaluated by three different methods, (**a**) ABTS, (**b**) DPPH, and (**c**) FRAP; and (**d**) total phenolic content (TPC) in leaves of *Capsicum annuum* seedlings. The values are the average of four repetitions. Means (n=4). Bars represent the standard deviation of the mean. Different letters indicate statistically significant differences between treatments ($p < 0.05$) according to Tukey's post hoc test.

Some published work describes the effects of ZnONPs on the antioxidant activities of chili plants and other varieties. For example, Sánchez Perez et al. [43] analyzed chili seedlings treated with ZnONPs suspensions in concentrations from 100-400 mg/L, finding that the antioxidant activity measured by DPPH in true leaves increased significantly compared to the control, increasing the antioxidant activity in proportion to the concentration used, similar to the data found in our experimentation. Likewise, García López et al. [11] evaluated the effects on chili seedlings in contact with ZnONPs, finding that the impact depended on the tissue analyzed. While adding nanoparticles to the plumule did not alter antioxidant activity, adding them to the radicle increased DPPH activity in a concentration-dependent manner. On the other hand, two different studies [13,44] measured DPPH radical activity in chili plants, monitored the fruit antioxidant activity, and reported an increase in this activity upon exposure to ZnONPs.

In general, there are references to studies that have characterised antioxidant activity in the genus *Capsicum* following exposure to ZnONPs. Most of these only measure activity using DPPH and/or TPC, with few studies performing multiple antioxidant activities simultaneously. For antioxidant activity measured by the ferric reducing antioxidant power (FRAP) assay, the effect of ZnO exposure on *Portulaca oleracea* L. plants was determined [45]. In this study, an increase in antioxidant activity was observed as a function of exposure concentration. However, the effect was significantly greater in plants exposed to nanoparticles than in those treated with bulk ZnO.

In Miliauskienė's study [46], the effect of ZnONPs on Swiss chard was evaluated using three methods to determine antioxidant activity, including the ABTS assay. A significant change was observed when nanoparticles with sizes between 35 and 45 nm were used. However, antioxidant

 doi:10.20944/preprints202601.0199.v1

parameters decreased when sizes of 18 nm and 80-200 nm were used. The latter size range coincides with those used in our research; however, the observed trend differs from our results.

It is important to note that very few studies have examined the effects of ZnONPs on *Capsicum* species worldwide, using antioxidant assays beyond DPPH and TPC. One of the few examples is the work of the García-López group [13], which determined the effect of foliar-applied nanoparticles on the antioxidant parameters of *Capsicum chinense* (habanero) fruits. In that study, an induced increase in antioxidant activity was observed, as determined by ABTS, DPPH, FRAP, and TPC assays, with increases of 16, 29, 33, and 2%, respectively. However, no significant differences were observed in this study with increasing nanomaterial concentration. Nevertheless, differences relative to controls treated with $ZnSO_4$ at equivalent concentrations were observed, with the increase in antioxidant activity not significantly greater than in the untreated control.

The study by Adnan et al. [47] showed a clear pattern of increased phenolic compound production, with the highest value recorded in *Capsicum annuum* L. plants foliarly treated with ZnONPs at 100 mg/L. These results agree with previous studies [11,48]. However, our results indicate that, at both nanoparticle concentrations evaluated, phenol concentration increased relative to the control. However, at the highest concentration (NP500), a decrease of 13% is observed compared to the lowest concentration (NP50). In addition, no significant differences were observed between the concentrations of the bulk material.

Several studies have investigated the antioxidant activity and total phenolic content (TPC) in plants treated with bulk and nano ZnO. Iziy et al. [45] reported that phenolic content and antioxidant capacity were higher in leaf extracts of *Portulaca oleracea L.* when exposed to ZnO nanoparticles (ZnO NPs) compared to the bulk form. The same trend was observed in soybean plants treated either by foliar application or soil supplementation, regardless of the application method [49].

All of these results suggest that the observed effects are closely related to the concentration and method of ZnO application, as well as to the plant species and its phenological stage.

3.4.2. Antioxidant Enzymes

Enzymatic antioxidants in the different treatments were evaluated by determining four enzymes (GPOX, APX, CAT and SOD) involved in antioxidant defense processes.

Regarding Guaiacol peroxidase (GPOX, EC 1.11.1.7), the results (Figure 6A) showed a general decrease in its activity in all treatments where seedlings were treated with zinc oxide, both in its nanoparticle (NP) and bulk (B) forms, compared to the control group. When analyzing the effects by concentration and form, at 50 mg/kg a marked difference was observed: the NP50 treatment showed a significant decrease of 46.4% in GPOX activity. In contrast, the B50 treatment showed a much smaller reduction of only 4.8% compared to the control group seedlings. For the highest concentrations (500 mg/kg), the decrease in activity was 33.5% for NP500 and 45.4% for B500. These findings suggest that the effect of zinc oxide on *C. annuum* seedlings is more noticeable in nanomaterials. For example, to achieve an equivalent decrease in GPOX activity, 50 mg/kg of ZnONPs is necessary, whereas 500 mg/kg of the bulk zinc oxide is required.

As for Ascorbate peroxidase (APX, EC 1.11.1.1) enzyme activity, the results showed a different response pattern to GPOX (Figure 6B). Interestingly, there was no difference in treatments B50 and NP500 with respect to the control. While a significant decrease in APX activity was observed only in the treatment with nanoparticles at a concentration of 50 mg/kg (NP50), where the activity was 12.2% lower compared to the control group. In contrast, treatment with 500 mg/kg ZnO in bulk form (B500) resulted in a 13.5% increase in the activity of this enzyme.

In the case of the enzyme catalase (CAT, EC 1.11.1.6), a general decrease in its activity was observed in all zinc oxide treatments compared to the control group, without a concentration-dependent effect (Figure 6C). Specifically, in nanomaterial-treated seedlings (NP50 and NP500), CAT activity exhibited an average decrease of 11.2%. On the other hand, in those treated with the bulk material (B50 and B500), the effect was more pronounced, decreasing on average by 38.6% relative to the control.

 doi:10.20944/preprints202601.0199.v1

As with CAT, for the enzyme Superoxide dismutase (SOD, EC 1.15.1.1), no concentration-dependent effect of ZnO on its activity was observed (Figure 6D). However, the impact was opposite across particle sizes. A marked decrease in SOD activity was observed in treatments with ZnONPs (NP50 and NP500), with reductions of up to 93.0% relative to the control group. In contrast, for the treatments with the bulk material (B50 and B500), SOD enzyme activity increased by almost twofold (94.6%) relative to the control. This shows a clear difference in the effect on this enzyme, being directly dependent on the particle size.

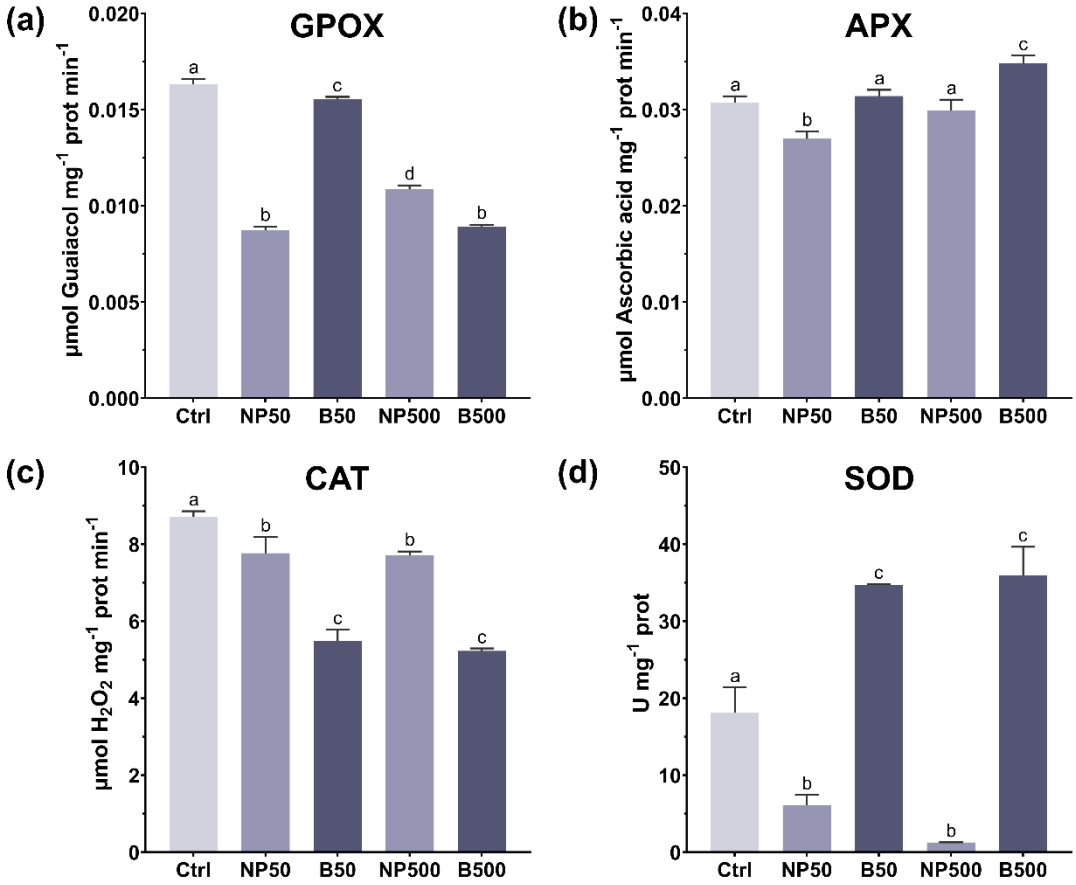

Figure 5. Effect of the application of nano (NP) and bulk (B) ZnO on activity of antioxidant enzyme (**a**) Guaiacol Peroxidase (GPOX), (**b**) Ascorbate Peroxidase (APX), (**c**) Catalase (CAT), and (**c**) Superoxide Dismutase (SOD) in leaves of *Capsicum annuum* seedlings. The values are the average of four repetitions. Means (n=4). Bars represent the standard deviation of the mean. Different letters indicate statistically significant differences between treatments ($p < 0.05$) according to Tukey's post hoc test.

The enzymatic response of plants to oxidative stress induced by zinc oxide nanoparticles (ZnONPs) is remarkably varied, depending on multiple factors.

Studies on monocotyledonous species, such as maize, have explored the effect of different concentrations of ZnONPs during germination. In these cases, the evaluation of the activity of enzymes such as GPOX, APX, CAT and SOD in stems and roots revealed an initial trend of increasing activities with increasing nanomaterial concentration. However, an inflection point (variable across enzymes and tissues) was observed, after which activities tended to decrease with increasing concentration. For example, catalase activity in maize roots increased at 50 and 100 mg/L ZnONPs, peaking before decreasing at 150 and 200 mg/L, and even reaching values lower than those of the control group [50]. In contrast to the results of our own study, where *C. annuum* seedlings were treated with ZnO in the substrate, other investigations on *C. annuum* L. plants foliar treated with ZnONPs have reported a general increase in the activity of enzymes such as SOD, APX, CAT and GPOX [19,47]. This difference underlines the importance of the exposure pathway as a determining

 doi:10.20944/preprints202601.0199.v1

factor in enzyme response. While in our study we observed mainly decreases in GPOX and CAT, and a mixed response in APX and SOD (with marked decreases in SOD for NPs but increases for the bulk form), foliar application seems to induce a generalized activation of these enzymes.

Concentration dependence has also been evidenced in other solanaceae, such as chile and tomato plants, where exposure to ZnONPs during germination (100 to 400 mg/L) led to a decrease in GPOX activity at treatments of 100 and 200 mg/L, emphasizing the importance of the concentrations employed [43].

Even within the same species, responses can vary markedly among genotypes. Such is the case of Don Pancho (DP) and Don Benito (DB) jalapeño chile varieties [18], foliar treated with nanoparticles. Although SOD activity showed an increasing trend in both varieties, CAT decreased in DP while it increased in DB. For APX, the trends were reversed, with an increase in DP and a decrease in DB.

Together, these results demonstrate that the effects of ZnONPs on crops are highly variable and multifactorial. The response of antioxidant enzymes depends not only on the concentrations and manner of application of the nanoparticles, but also on the plant species, its phenological stage and, crucially, the specific genotype within the same species. Understanding this complexity is essential to assess the real impact of nanomaterials on plant physiology.

3.5. Volatiles Analysis

For the analysis of volatile organic compounds (VOCs), solid-phase microextraction (SPME) was used, following the conditions detailed in the methodology. The VOCs extracted in the fiber were desorbed and analyzed by gas chromatography coupled to mass (GC-MS).

In order to perform an initial screening and compare the diversity and abundance of VOCs, a global analysis was carried out. Those compounds with an abundance of at least 1300 arbitrary units (A.U.) in the chromatograms and showing distinct fragmentation patterns were considered.

To facilitate the interpretation of these results, a Venn diagram (Figure 7) was generated to illustrate the grouping of differential and shared compounds between treatments. This diagram clearly identifies the differences in chemical composition diversity among them.

Plants treated with ZnONPs at a concentration of 500 mg/kg (NP500) showed the highest diversity, with a total of 61 volatile compounds detected, of which 10 were unique to this treatment (Figure 7). In contrast, the rest of the treatments exhibited similar behavior to each other, with between 45 and 47 compounds detected in each. The treatments with 50 mg/kg of both nanometric (NP50) and bulk (B50) forms of zinc oxide showed the same number of VOCs and the same number of unique compounds.

 doi:10.20944/preprints202601.0199.v1

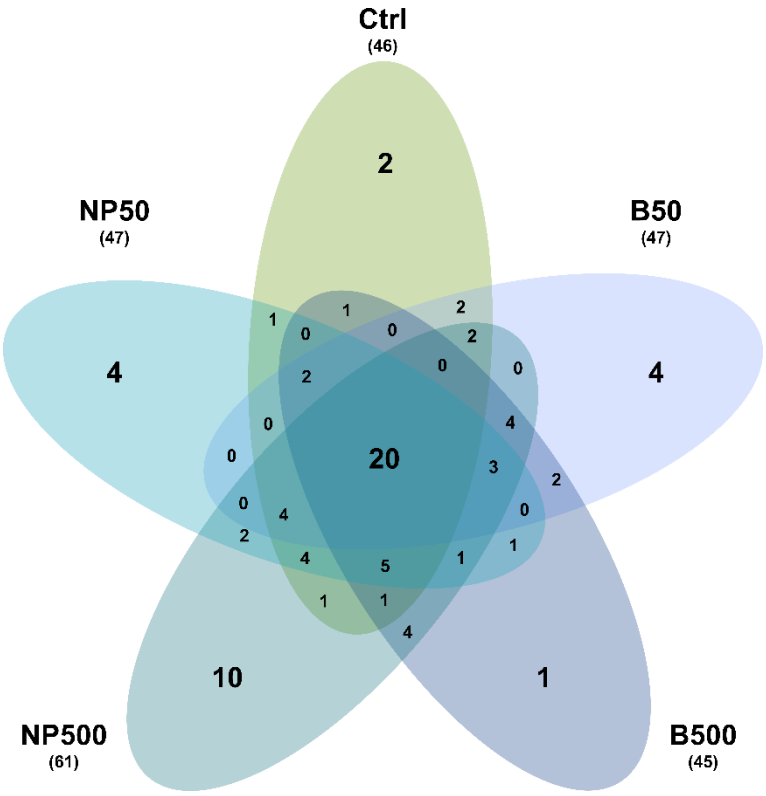

Figure 7. Venn diagram of the number of unique and shared volatile compounds among *Capsicum annuum* seedlings of the different treatments.

The increase in diversity presented in the NP500 treatment agrees with previous studies, such as that of Piesik et al. [51] who observed a stimulation in the production and an increase in the concentration of VOCs in Brassica napus plants treated with iron nanoparticles and elicitors, compared to those treated only with elicitors, showing a response in the increase in the concentration of VOCs dependent on the concentration of the nanoparticles.

Following this initial analysis, a second screening of VOCs was conducted. For this, compounds in each sample that met two criteria were selected:

Confirmation of identity: verified by comparing the experimental Kovats retention index with values reported in the literature, with a variation of no more than 10 units.

Abundance: They had to exhibit a relative abundance of at least 1.0% in at least one treatment.

These screened compounds are detailed in Table 3. The VOCs identified belong to various groups of molecules, including aldehydes and six-carbon alcohols, esters, terpenes, and aromatic compounds and their derivatives.

Table 3. Relative abundance of volatile compounds identified in *C. annuum* seedlings under the different treatments.

			% Area						
Name	**FM[1]**	**MM[2]**	**Ctrl**	**NP50**	**B50**	**NP500**	**B500**	**IK(exp) [3]**	**IK(lit) [4]**
(Z)-3-Hexenal	$C_6H_{10}O$	98.1	3.5	7.5	12.7	-	1.2	792.7	799.5
n-Hexanal	$C_6H_{12}O$	100.2	5.7	7.9	4.4	6.9	12.7	794.3	793.0
(E)- 2-Hexenal	$C_6H_{10}O$	98.1	11.4	11.9	12.9	8.1	6.1	854.2	854.0
(Z)-3-Hexenol	$C_6H_{12}O$	100.2	7.7	11.1	9.2	5.7	3.3	858.6	858.0
(E)-2-Hexenol	$C_6H_{12}O$	100.2	3.9	3.6	2.0	0.8	0.5	869.3	869.0

 doi:10.20944/preprints202601.0199.v1

p-Xylene	C_8H_{10}	106.2	-	-	-	2.1	0.8	869.7	865.0
n-Hexanol	$C_6H_{14}O$	102.2	8.0	4.3	6.7	-	2.2	871.3	871.0
(Z)-3-Hexenyl Acetate	$C_8H_{14}O_2$	142.2	15.9	14.4	7.3	9.0	0.8	1005.2	1007.0
n-Hexyl Acetate	$C_8H_{16}O_2$	144.2	2.7	1.9	0.8	1.0	-	1012.4	1012.0
2-Hexenyl Acetate	$C_8H_{14}O_2$	142.2	3.5	3.7	0.5	1.4	-	1015.4	1017.0
Indene	C_9H_8	116.2	0.1	1.3	-	0.03	-	1046.5	1051.0
Linalool	$C_{10}H_{18}O$	154.2	1.4	-	0.05	-	-	1097.8	1098.0
n-Nonanal	$C_9H_{18}O$	142.2	1.1	1.7	3.4	4.9	3.8	1102.2	1102.0
Methyl Salicylate	$C_8H_8O_3$	152.1	24.4	12.0	0.2	16.6	41.7	1196.9	1196.0
n-Decanal	$C_{10}H_{20}O$	156.3	0.5	1.2	2.8	3.5	2.6	1204.0	1204.0
2-Ethyl-3-hydroxyhexyl-2-methylpropanoate	$C_{12}H_{24}O_3$	216.3	0.5	1.3	0.1	2.8	2.3	1377.3	1373.0
n-Decyl Acetate	$C_{12}H_{24}O_2$	200.3	-	1.4	-	0.5	-	1406.2	1408.0
β-Farnesene	$C_{15}H_{24}$	204.4	-	-	17.0	-	1.3	1457.1	1457.0
1-Dodecanol	$C_{12}H_{26}O$	186.3	0.9	3.0	1.0	3.4	3.4	1472.3	1472.0
2,2,4-Trimethyl-1,3-pentanediol diisobutyrate	$C_{16}H_{30}O_4$	286.4	0.6	1.7	-	3.9	1.9	1597.4	1587.5
α-Bisabolol	$C_{15}H_{26}O$	222.4	0.3	-	-	2.9	1.1	1675.8	1685.0
2-Ethylhexyl salicylate	$C_{15}H_{22}O_3$	250.3	0.2	0.4	-	1.0	0.8	1810.9	1812.0
Isopropyl myristate	$C_{17}H_{34}O_2$	270.5	-	-	0.1	1.2	0.3	1821.4	1823.0

(1)FM: Molecular formula. (2)MM: Molecular mass (Atomic mass units). (3)IK_{exp}: Kovats indices calculated from retention times on a *HP-5ms Ultra Inert* column. (4)IK_{lit}: Kovats index from the *NIST Chemistry Web Book* [52].

When analyzing the data in the table, we observed that methyl salicylate was the predominant compound across most treatments. The only exception was treatment B50, in which β-farnesene was identified as the primary compound.

In the control group, methyl salicylate accounted for 24.4% of the relative abundance. However, a decrease in the abundance of this compound was observed in treatments NP50 and NP500, at 12% and 16.6%, respectively. Interestingly, treatment B500 exhibited a significant increase in the relative abundance of methyl salicylate compared to the control, reaching 41.7%. Methyl salicylate is a volatile phenolic compound of great importance in plants. One of its primary functions is to act as a long-distance signaling molecule, facilitating communication among plants and inducing a collective response. Its biosynthesis is caused by various abiotic stresses, including drought, high soil salinity, and elevated temperatures [53,54]. In addition, methyl salicylate has been observed to modulate the production of other volatile compounds in the plant.

An example is the work of Liu et al. [55], who demonstrated that treating birch plants with varying concentrations of methyl salicylate increased the production of volatile terpenoids and certain benzene derivatives. Taken together, our results indicate that the form of Zn used in the treatment modulates the methyl salicylate response. Specifically, treatments with zinc nanoparticles

 doi:10.20944/preprints202601.0199.v1

(NP50 and NP500) significantly reduced methyl salicylate production, whereas bulk Zn (B500) increased its levels. To our knowledge, no studies have linked this decrease in the methyl salicylate-mediated response in plants exposed to nanoparticles; therefore, this finding warrants further investigation.

On the other hand, methyl salicylate was present at only 0.2% abundance in the B50 treatment, whereas other signaling- and defense-related compounds showed increased abundance. For example, β-farnesene, a sesquiterpene known for its role in indirect plant defense, was detected and identified only in the bulk ZnO treatments, with abundances of 17.0 and 1.3% for B50 and B500, respectively. This could indicate suppression or reorientation of metabolic pathways due to the presence of ZnO in bulk form.

To effectively visualize and compare the results, a heat map (Figure 8) was generated, showing the relative abundance of the remaining volatile compounds identified.

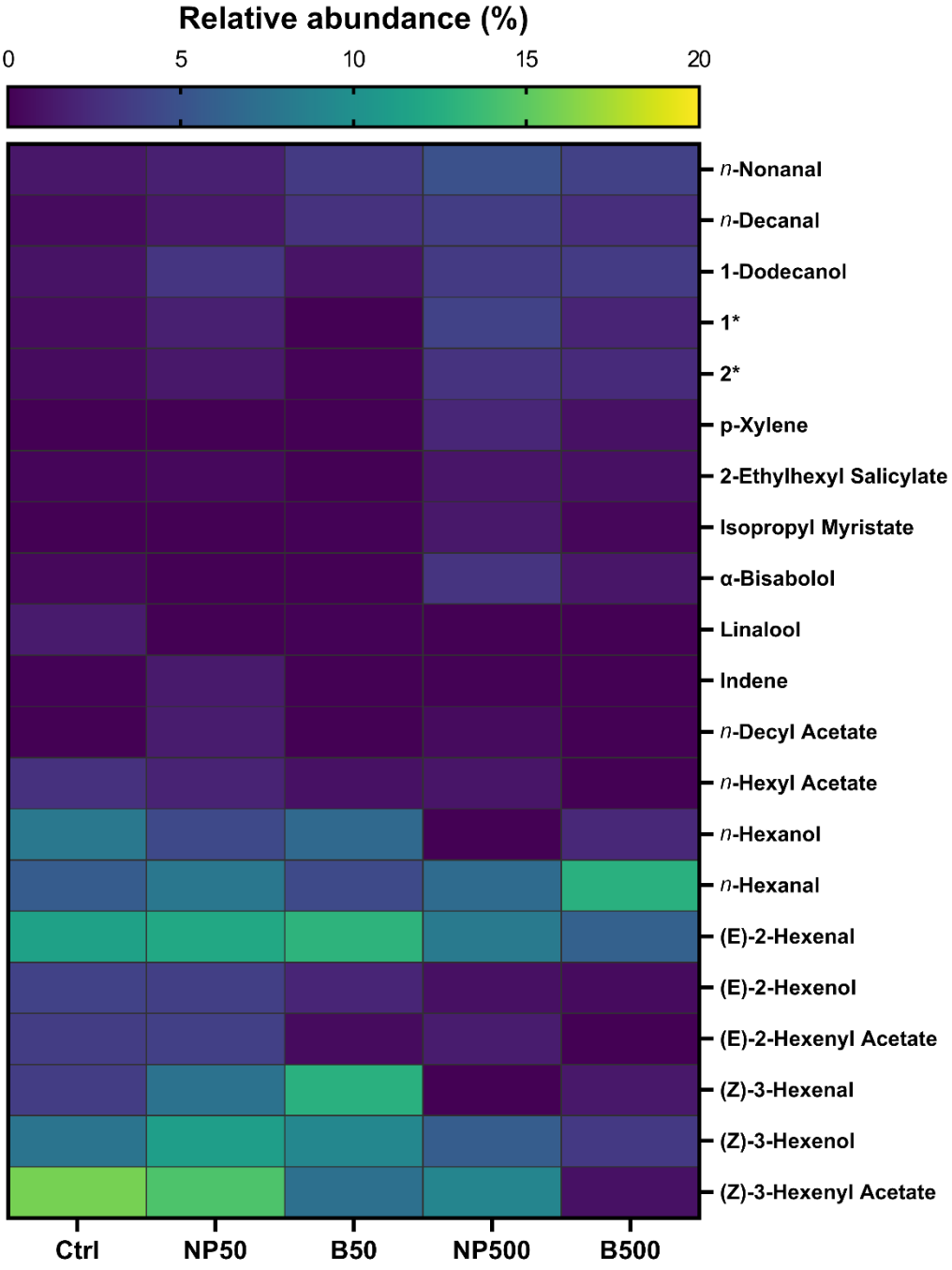

 doi:10.20944/preprints202601.0199.v1

Figure 8. Heat map relative abundance of the volatile compounds (VOCs) identified in seedlings of *Capsicum annuum*. Compounds with abbreviated names in the figure correspond to 1*: 2,2,4-Trimethyl-1,3-pentanediol diisobutyrate; 2*: 2-ethyl-3-hydroxyhexyl 2-methylpropanoate.

In the terpenoid category, it was observed that the production of linalool, a monoterpene, was inhibited in the ZnONPs treatments and at the highest concentration of bulk ZnO. This compound was present only in the control (1.4%) and B50 (0.05%). On the other hand, for α-bisabolol, a sesquiterpene, an increase in its production was observed at the highest ZnO concentrations in both forms. This compound was absent at low concentrations (NP50, B50), but appeared at NP500 (2.9%) and B500 (1.1%), in contrast to the control (0.3%). The decrease and increase of the different terpenoids in response to the different ZnO treatments suggest an alteration in this biosynthetic pathway as part of the defense or stress response of the seedlings.

Long-chain aldehydes such as nonanal and decanal were present in all treatments, with a general tendency for their relative abundance to increase at higher ZnO concentrations. It is well established that aldehyde production in plants occurs primarily via lipid peroxidation, a process induced by free radicals. These aldehydes are formed by fragmentation of the resulting lipoperoxides, which generate compounds of various chain lengths [56]. This suggests that the increased production of nonanal and decanal could be a response of seedlings to oxidative stress induced by the incorporation of zinc oxide into the growing soil.

Additionally, specific appearance patterns were observed for other volatile compounds. On the one hand, decyl acetate was detected exclusively in treatments with zinc oxide nanoparticles (ZnONPs). On the other hand, compounds such as p-Xylene (present in NP500: 2.1% and B500: 0.8%) and isopropyl myristate (identified at the highest concentrations: NP500: 1.2% and B500: 0.3%) were detected to a greater extent in treatments with high concentrations, being absent in the control. The presence of these metabolites could indicate their induction in response to stress conditions associated with high ZnO concentrations in the growing soil.

Continuing the characterization of volatile compounds emitted by the seedlings, a group of compounds of particular relevance to stress and defense signaling was identified. These are the Green Leaf Volatiles (GLVs) (Scala et al., 2013). Their biosynthesis, illustrated in detail in Figure 9, initiates with the action of lipoxygenases (LOX) on fatty acids such as α-linolenic and linoleic acids, forming hydroperoxides. These are subsequently fragmented by hydroperoxide lyases (HPLs) into 6-carbon aldehydes, which can then be isomerized or reduced to alcohols and acetylated, thereby generating the diversity of GLVs [57].

Starting with the linoleic acid-derived GLVs, for hexanal, a pattern of increase is observed in most treatments, NP50, NP500, and B500, where relative abundance values of 7.9, 6.9, and 12.7% were obtained, respectively, compared to the control group, where only 5.7% was obtained. The only treatment to show a decrease in this compound was the seedlings of group B50, which showed 4.4%. Continuing with the route, a marked pattern is observed in the behavior of the sequential compounds of this metabolic process, hexanol and hexanyl acetate. In both cases, production is reduced or suppressed, as in NP500 for hexanol and B500 for hexenyl acetate. These results suggest a concentration-dependent inhibitory effect of cinnamaldehyde and hexanal reductase (CHR) by the presence of zinc oxide in the substrate, thus explaining the increase in the abundance of hexanal, due to its accumulation because it cannot follow its transformation in the biosynthetic pathway.

Continuing with the α-linolenic acid pathway, the same pattern is observed for (Z)-3-hexenal and (E)-2-hexenal, with both compounds showing an increase in their production for the lowest concentration treatments, NP50 and B50. However, these compounds show a decrease at the highest concentrations of zinc oxide in the substrate (NP500 and B500). This behavior suggests modulation of the pathway: it is stimulated at low ZnO concentrations and inhibited at higher concentrations.

Turning to the subsequent compounds of the pathway, in the case of (Z)-3-hexenol the previous behavior in the pathway is maintained, by increasing the production of this compound in the treatments with low concentrations, NP50 and B50, and observing a decrease in the abundance in the

 doi:10.20944/preprints202601.0199.v1

NP500 and B500 treatments with respect to the control. In contrast, its isomer, (E)-2-hexenol, showed a concentration-dependent decrease in production in all treatments. This pattern agrees with the results obtained in the linoleic acid pathway, where inhibition of the CHR enzyme is hypothesized.

Finally, for compounds (Z)-3-hexenyl acetate and (E)-2-hexenyl acetate, their decrease is observed in all cases, with the exception of the (E) isomer in the NP50 treatment, where only a 0.2% increase is shown with respect to the control group.

With these results, it can be inferred that the treatment of *C. annuum* seedlings with zinc oxide stimulates the linoleic acid degradation pathway, as well as the inhibition of the enzymatic processes where the enzyme cinnamaldehyde and hexanal reductase are involved, seeing the most marked effect in high concentrations of ZnO and in the biosynthetic processes of hexanal and (E)-2-hexenal.

Little information is available on the effects of nanomaterials on the production of volatiles in plants, and even less is known about specific compounds such as the GLV group.

Recent research, such as that of Piesik et al. [51], demonstrates a stimulatory effect of iron nanoparticles (FeNPs) on the production of some GLVs and their derivatives, specifically for (Z)-3-hexenal, (E)-2-hexenal, (Z)-3-hexenol and (Z)-3-hexenyl acetate. For these compounds, a trend of increasing concentration-dependent production of FeNPs was observed. However, in our investigation, the effect on GLVs was heterogeneous, indicating that effects and mechanisms of action depend on the nature of the material and other variables.

 doi:10.20944/preprints202601.0199.v1

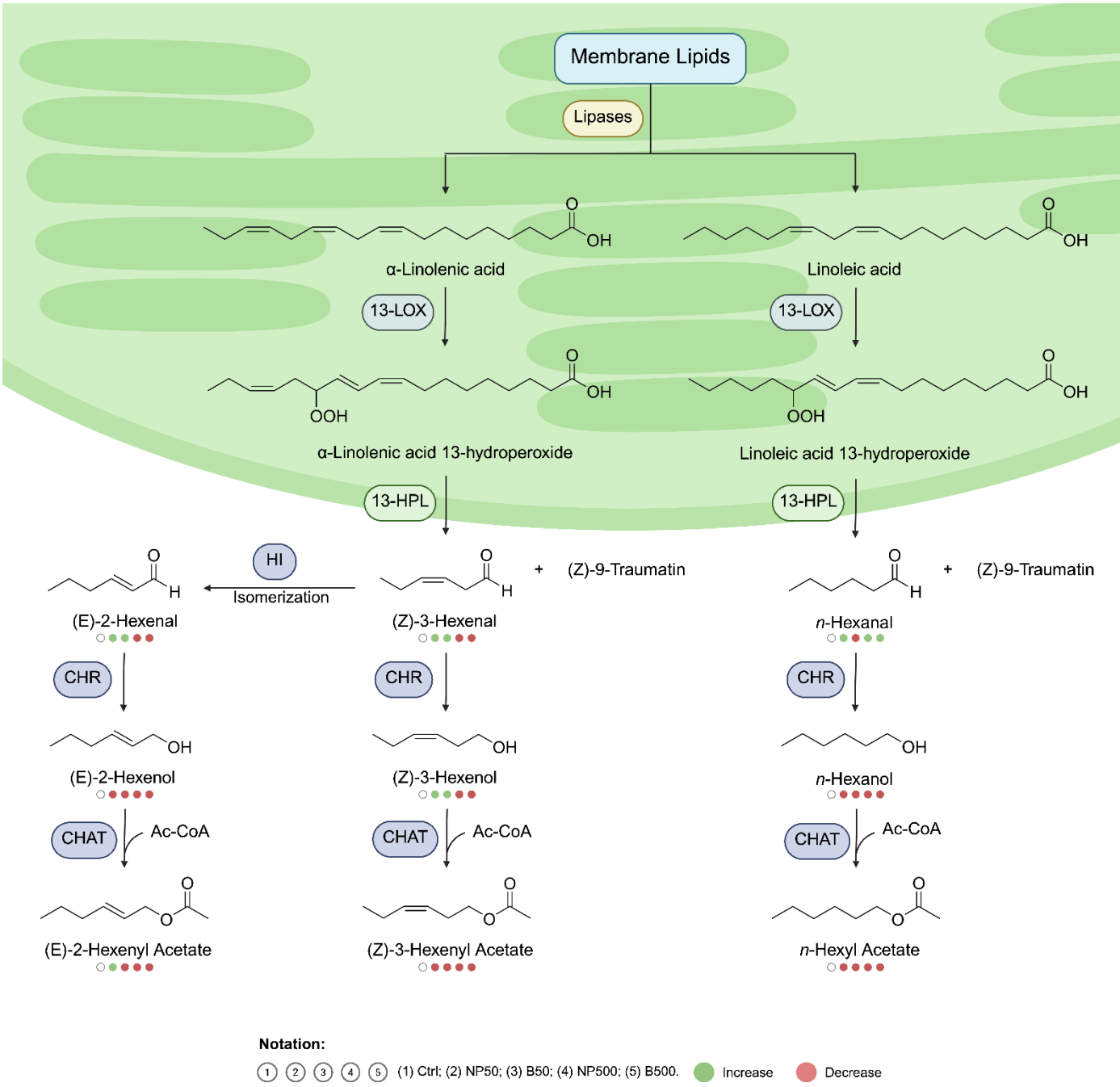

Figure 9. Metabolic pathway of the formation of green leaf volatiles from the peroxidation of polyunsaturated fatty acids.

4. Discussion

The interaction between nanomaterials and plant biological systems is a multifaceted phenomenon where understanding dose-response toxicology is a challenge. In this study, by contrasting the effects of zinc oxide nanoparticles (ZnONPs) versus ZnO (Bulk) on *Capsicum annuum* seedlings, we have identified a series of divergent physiological, metabolic, and ecological responses that suggest different mechanisms of action depending on the scale of the material. The results reveal that, although both materials supply zinc to the plant, ZnONPs induce a specific modification of the antioxidant machinery, a selective blockage in volatile signalling pathways and a restructuring of the phyllosphere microbiome.

 doi:10.20944/preprints202601.0199.v1

A counterintuitive finding of this study was that, at high concentrations (500 mg kg^{-1}), treatment with bulk ZnO (B500) resulted in higher foliar zinc accumulation (128.7 mg kg^{-1}) compared to treatment with nanoparticles (NP500, 119.7 mg kg^{-1}). 1 This result contradicts the idea that nanoparticles, being smaller in size, tend to be more bioavailable and have better cellular absorption. However, this behaviour is consistent with the colloidal chemistry of nanoparticles in complex edaphic matrices. Recent studies, such as those by Kim et al. [39] and other authors [58], suggest that at high concentrations, ZnONPs undergo rapid agglomeration in soil, forming micrometric clusters that drastically reduce their specific surface area and dissolution rate. In addition, ZnONPs can interact strongly with organic matter and clays in the substrate, becoming immobilised or forming insoluble complexes (zinc phosphates) that limit their root absorption [59].

In contrast, bulk ZnO particles, although initially larger, can dissolve more slowly but steadily, releasing Zn^{2+} ions that are efficiently captured by high- and low-affinity transporters in the root. 28 Therefore, it is plausible that the higher bioaccumulation in treatment B500 reflects a higher net availability of Zn^{2+} ions in the soil solution over time, while ZnONPs remained retained in the soil matrix or on the root surface without being effectively internalized.

In terms of changes in enzyme activities, the response of Superoxide Dismutase (SOD) represents the most critical physiological point of divergence between treatments. While Bulk ZnO stimulated SOD activity (an expected defense mechanism against metal stress), ZnONPs caused nearly complete inhibition of the enzyme (a 93% decrease). It has been documented that nanoparticles can bind to enzyme active sites or induce conformational changes ('unfolding') that inactivate their catalytic function [60,61]. Regardless of the mechanism, the functional outcome for the plant is a state of antioxidant vulnerability under NP treatments, corroborated by a concomitant decrease in other enzymes, such as Catalase (CAT) and guaiacol peroxidase (GPOX). This forces the plant to rely on non-enzymatic defenses, explaining the observed increase in total phenols and antioxidant capacity (DPPH/ABTS) as a compensatory mechanism [43,50].

On the other hand, the volatile compound (VOC) profile revealed a profound and specific metabolic disturbance induced by ZnONPs, affecting two crucial pathways: Green Leaf Volatiles (GLVs) and the Salicylic Acid pathway. GLVs are generated after stress via the lipoxygenase (LOX) pathway, where membrane fatty acids are oxidized to hydroperoxides, cleaved by hydroperoxide lyase (HPL) to C6 aldehydes (e.g., hexanal), and finally reduced to alcohols (e.g., hexanol) by alcohol dehydrogenase (ADH) [62]. Our results show a significant accumulation of Hexanal and a suppression of Hexanol and Hexyl Acetate in the zinc treatments. This pattern of substrate accumulation/product depletion indicates inhibition of the ADH enzyme. Although zinc is a structural cofactor of ADH, supraphysiological concentrations of heavy metals or direct interaction with nanoparticles can inhibit its activity by distorting the catalytic site or oxidizing essential thiol groups [63,64].

The most striking finding is the divergence in MeSA emission. While the Bulk treatment (B500) elevated MeSA to 41.7% of the volatile profile (indicative of strong Activated Systemic Resistance - SAR), ZnONPs (NP500) suppressed its emission to 16.6%.

MeSA is synthesised from salicylic acid (SA) by the enzyme Salicylic Acid Carboxyl Methyl Transferase (SAMT) [65]. The observed suppression suggests that ZnONPs inhibit SAMT activity or gene expression. This could be due to transcriptional reprogramming induced by the unique oxidative stress of NPs, implying that treated plants may be less able to alert their neighbours to pathogen attacks, compromising the population immunity of the crop, a side effect not observed with conventional zinc fertilizer [66–68].

Finally, metagenomic analysis revealed that, although alpha diversity (Shannon/Simpson indices) remained stable, taxonomic composition underwent directional changes under zinc pressure. A notable increase in the relative abundance of the phylum Actinobacteria was observed in treatments with high doses of zinc (especially B500).1 Actinobacteria are recognized for their extraordinary metabolic versatility, sporulation capacity and intrinsic resistance to heavy metals and oxidative stress [69]. Their enrichment suggests that the zinc-rich environment of the phylosphere

 doi:10.20944/preprints202601.0199.v1

acts as a severe selective filter, favouring those microorganisms genetically equipped with metal efflux pumps and robust antioxidant systems [70].

On the other hand, the detection and subsequent decrease in Spirochaetes under zinc treatments are intriguing findings [71]. Although this phylum is atypical in the phylosphere (commonly associated with anaerobic or animal environments), its basal presence in the control and its reduction with treatment confirm the known sensitivity of spirochetes to heavy metals and oxidizing conditions. The decrease in this group, together with the stability of the dominant phylum Proteobacteria, indicates that ZnONPs cause selective dysbiosis by eliminating sensitive taxa [72].

Taken together, these results indicate that ZnONPs do not act merely as fertilizers but rather as multifactorial stressors. At the intracellular level, they cause a redox imbalance that inactivates key enzymes (SOD, ADH). At the systemic level, they alter chemical communication (suppression of MeSA, blocking of GLVs). And at the ecological level, they remodel the associated microbial community (increase in Actinobacteria).

The fundamental difference with bulk ZnO lies in the intensity and specificity of these effects. While Bulk activates classic defence mechanisms (elevated SOD and MeSA), NPs appear to attenuate these systems, forcing the plant into alternative metabolic states. This highlights the need to evaluate agricultural nanomaterials not only for their effect on yield (biomass), but also for their invisible impact on the physiological and ecological resilience of the crop.

5. Conclusions

This research demonstrates that the application of zinc oxide nanoparticles (ZnONPs) in *Capsicum annuum* elicits divergent physiological and molecular responses compared with their micrometric counterpart (ZnOBulk). Despite the theoretical properties of nanomaterials, ZnONPs exhibited significantly lower foliar bioavailability at 500 mg kg^{-1}, a phenomenon attributed to particle agglomeration in the substrate, which restricts ionic dissolution and subsequent root absorption. In the enzymatic sphere, the Bulk material stimulated superoxide dismutase SOD activity. At the same time, ZnONPs caused severe enzymatic inhibition, attributable to direct structural inactivation via nanoparticle internalization, thereby compromising homeostatic responses to oxidative stress. Likewise, a substantial alteration in the profile of volatile organic compounds was observed, likely due to the inhibition of certain enzymes and the resulting accumulation of hexanal. This metabolic disruption extended to the suppression of methyl salicylate MeSA, altering the systemic resistance mechanisms and interplant signalling. Finally, exposure to zinc restructured the taxonomic composition of the phyllosphere through selective pressure, favouring the proliferation of Actinobacteria and the exclusion of sensitive taxa, representing a significant modification in the ecological dynamics of the leaf microbiome.

Author Contributions: Conceptualization, L.A.G.-C. and G.V.-J.; methodology, O.K.R.-M. and L.A.G.-C.; validation, C.R.C.-Á. and R.E.G.; investigation, A.Z.-O.; data curation, R.S.-F. and L.A.G.-C.; writing—original draft preparation, L.A.G.-C., V.Z.M. and G.V.-J.; writing—review and editing, J.S.G.-M. and G.V.-J.; project administration, G.V.-J. and D.A.L.-R.; funding acquisition, G.V.-J. and D.A.L.-R. All authors have read and agreed to the published version of the manuscript.

Funding: This research was funded by Secretaría de Ciencia, Humanidades, Tecnología e Innovación (Secihti), grant number CF-2023-G-728, "Impacto de las nanopartículas en el cultivo del chile (Capsicum annuum, L.)".

Institutional Review Board Statement: Not applicable.

Informed Consent Statement: Not applicable.

Data Availability Statement: The data presented in this study are available within the article.

Acknowledgments: The authors thank the Laboratorio Nacional de Investigación y Servicio Agroalimentario y Forestal (LANISAF), Colegio de Postgraduados, and Universidad Autónoma Chapingo for providing access to their facilities and technical support during the development of this research.

 doi:10.20944/preprints202601.0199.v1

Conflicts of Interest: The authors declare no conflicts of interest.

References

1. Díaz-Parra DG, García-Casillas LA, Velasco-Ramírez SF, Guevara-Martínez SJ, Zamudio-Ojeda A, Zuñiga-Mayo VM, et al. Role of Metal-Based Nanoparticles in Capsicum spp. Plants. ACS Omega. 2025;10(11):10756–68.
2. Food and Agriculture Organization of the United Nations. FAOSTAT – Production: Crops and livestock products (Chillies and peppers) [Internet]. 2024 [cited 2025 Sept 10]. Available from: https://www.fao.org/faostat/en/#data/QCL
3. Liu F, Zhao J, Sun H, Xiong C, Sun X, Wang X, et al. Genomes of cultivated and wild Capsicum species provide insights into pepper domestication and population differentiation. Nature Communications. 2023;14(1).
4. Carrizo García C, Barfuss MHJ, Sehr EM, Barboza GE, Samuel R, Moscone EA, et al. Phylogenetic relationships, diversification and expansion of chili peppers (Capsicum, Solanaceae). Annals of Botany. 2016;118(1):35–51.
5. Batiha GE saber, Alqahtani A, Ojo OA, Shaheen HM, Wasef L, Elzeiny M, et al. Biological Properties , Bioactive Constituents , and Pharmacokinetics of Some Capsicum spp . and Capsaicinoids. International Journal of Molecular Sciences. 2020;21:5179.
6. Hernández-Pérez T, Gómez-García M del R, Valverde ME, Paredes-López O. Capsicum annuum (hot pepper): An ancient Latin-American crop with outstanding bioactive compounds and nutraceutical potential. A review. Comprehensive Reviews in Food Science and Food Safety. 2020 Nov;19(6):2972–93.
7. Zemanov V, Pavl D, Nov M, Hnilič F. The Dual Role of Zinc in Spinach Metabolism : Beneficial × Toxic. Plants. 2024;13:3363.
8. Guzel A, Sertan D, Oskay Ç, Ersan K, Ayşegül T, Rıza Y. Effects of green and chemically synthesized ZnO nanoparticles on Capsicum annuum under drought stress. Acta Physiologiae Plantarum. 2025;47(2):1–17.
9. Khan AR, Xingming A, Zaid F, Abdul U, Muhammad S, Yihua A. Efficacy of zinc - based nanoparticles in alleviating the abiotic stress in plants : current knowledge and future perspectives. Environmental Science and Pollution Research. 2023;30:110047–68.
10. Ravishankar TN, Ananda A, Shilpa BM, Adarsh J. Eco-friendly synthesis of NiO and Ag / NiO nanoparticles : applications in photocatalytic and antibacterial activities. Royal Society Open Science. 2025;12:241733.
11. García-López JI, Lira-saldivar RH, Zavala- F, Olivares-sáenz E, Niño-medina G, Ruiz- NA, et al. Effects of zinc oxide nanoparticles on growth and antioxidant enzymes of Capsicum chinense. Toxicological & Environmental Chemistry [Internet]. 2018; Available from: http://dx.doi.org/10.1080/02772248.2018.1550781
12. García-López JI, Zavala-Garcia F, Olivares-Saénz E, Lira-Saldivar RH, Barriga-Castro ED, Ruiz-Torres NA, et al. Zinc Oxide nanoparticles boosts phenolic compounds and antioxidant activity of capsicum annuum l. during germination. Agronomy. 2018 Oct;8(10):215.
13. García-López JI, Niño-Medina G, Olivares-Sáenz E, Lira-Saldivar RH, Barriga-Castro ED, Vázquez-Alvarado R, et al. Foliar Application of Zinc Oxide Nanoparticles and Zinc Sulfate Boosts the Content of Bioactive Compounds in Habanero Peppers. Plants 2019, Vol 8, Page 254. 2019 July;8(8):254.
14. Dileep Kumar G, Raja K, Natarajan N, Govindaraju K, Subramanian KS. Invigouration treatment of metal and metal oxide nanoparticles for improving the seed quality of aged chilli seeds (Capsicum annum L.). Materials Chemistry and Physics. 2020 Feb;242:122492.
15. Younes NA, Hassan HS, Elkady MF, Hamed AM, Dawood MFA. Impact of synthesized metal oxide nanomaterials on seedlings production of three Solanaceae crops. Heliyon. 2020;6:e03188.
16. Ghareeb RY, Belal EB, El-Khateeb NMM, Shreef BA. Utilizing bio-synthesis of nanomaterials as biological agents for controlling soil-borne diseases in pepper plants: root-knot nematodes and root rot fungus. BMC Plant Biology. 2024 Dec;24:110.

 doi:10.20944/preprints202601.0199.v1

17. Kumar R, Pratap S, Fedor S, Aleksey I, Maksimov Y, Latsynnik E. Trichoderma -Mediated Synthesis of ZnONPs : Trend Efficient for Repressing Two Seed- and Soil-Borne Phytopathogens Phomopsis vexans and Colletotrichum capsici. BioNanoScience. 2024;14:5363–76.
18. Rivero-montejo SDJ, Rivera-bustamante RF, Saavedra-trejo DL, Vargas-hernandez M, Palos-barba V, Macias-bobadilla I, et al. Plant Physiology and Biochemistry Inhibition of pepper huasteco yellow veins virus by foliar application of ZnO nanoparticles in Capsicum annuu m L. Plant Physiology and Biochemistry. 2023;203:108474.
19. Rasouli F, Asadi M, Hassanpouraghdam MB, Aazami MA, Ebrahimzadeh A, Kakaei K, et al. Foliar Application of ZnO-NPs Influences Chlorophyll Fluorescence and Antioxidants Pool in Capsicum annum L. under Salinity. Horticulturae. 2022 Oct;8(10):908.
20. Karmous I, Gammoudi N, Chaoui A. Assessing the Potential Role of Zinc Oxide Nanoparticles for Mitigating Cadmium Toxicity in Capsicum annuum L. Under In Vitro Conditions. Journal of Plant Growth Regulation. 2023 Feb;42(2):719–34.
21. Irfan SM, Bhatti KH. Zinc Oxide Nanoparticles Mitigate Toxic Effects of Cadmium Heavy Metal in Chilli (Capsicum annuum L.). Proceedings of the Pakistan Academy of Sciences: Part B. 2023;60(3):477–87.
22. Matsui K, Engelberth J. Green Leaf Volatiles — The Forefront of Plant Responses Against Biotic Attack Special Issue – Review. Plant and Cell Physiology. 2022;63(10):1378–90.
23. Simpraga M, Takabayashi J, Holopainen JK. Language of plants : Where is the word? Journal of integrative plant biology. 2016;58(4):343–9.
24. Engelberth J. Primed to grow : a new role for green leaf volatiles in plant stress responses. Plant Signaling & Behavior. 2020;15(1):e1701240.
25. Huang Y, Jiang J, Wang Y, Chen J, Xi J. Nanozymes as Enzyme Inhibitors. International journal of nanomedicine. 2021;16:1143–55.
26. Chen H, Song Y, Wang Y, Wang H, Ding Z, Fan K. Zno nanoparticles : improving photosynthesis , shoot development , and phyllosphere microbiome composition in tea plants. Journal of Nanobiotechnology. 2024;238.
27. Rangel LI, Leveau JHJ. Applied microbiology of the phyllosphere. Applied Microbiology and Biotechnology. 2024;108:211.
28. Sirelkhatim A, Mahmud S, Seeni A. Review on Zinc Oxide Nanoparticles : Antibacterial Activity and Toxicity Mechanism. Nano-Micro Letters. 2015;7(3):219–42.
29. Stratil P, Klejdus B, Kubáň V. Determination of Total Content of Phenolic Compounds and Their Antioxidant Activity in Vegetables s Evaluation of Spectrophotometric Methods. Journal of Agricultural and Food Chemistry. 2006;54:607–16.
30. Brand-Williams W, Cuvelier ME, Berset C. Use of a Free Radical Method to Evaluate Antioxidant Activity. LWT - Food Science and Technology. 1995;28:25–30.
31. Benzie IFF, Strain JJ. The Ferric Reducing Ability of Plasma (FRAP) as a Measure of " Antioxidant Power ": The FRAP Assay. Analytical Biochemistry. 1996;76:70–6.
32. Singleton VL, Rossi JA. Colorimetry of Total Phenolics with Phosphomolybdic-Phosphotungstic Acid Reagents. Am J Enol Vitic. 1965;16(16):144–58.
33. Castillo FJ, Penel C, Greppin H. Peroxidase Release Induced by Ozone in Sedum album Leaves. Plant Physiology. 1984;74:846–51.
34. Nakano Y, Asada K. Hydrogen Peroxide is Scavenged by Ascorbate-specific Peroxidase in Spinach Chloroplasts. Plant and Cell Physiology. 1981;22(5):867–80.
35. Dhindsa RS, Plumb-dhindsa P, Thorpe TA. Leaf Senescence: Correlated with Increased Levels of Membrane Permeability and Lipid Peroxidation, and Decreased Levels of Superoxide Dismutase and Catalase. Journal of Experimental Botany. 1981 Feb;32(1):93–101.
36. Lucero M, Estell R, Fredrickson E. A Retention Index Calculator Simplifi es Identifi cation of Plant Volatile Organic Compounds. Phytochemical Analysis. 2009;20:378–84.
37. Zhang D, Hua T, Xiao F, Chen C, Gersberg RM, Liu Y, et al. Phytotoxicity and bioaccumulation of ZnO nanoparticles in Schoenoplectus tabernaemontani. Chemosphere. 2015 Feb;120:211–9.

 doi:10.20944/preprints202601.0199.v1

38. Cruz TNM, Savassa SM, Montanha GS, Ishida JK, Almeida ED, Tsai SM, et al. A new glance on root-to-shoot in vivo zinc transport and time- dependent physiological effects of ZnSO 4 and ZnO nanoparticles on plants. Scientific Reports. 2019;9(May):10416.
39. Hoon S, Bae S, Woo Y, Sik Y. Effects of particle size on toxicity , bioaccumulation , and translocation of zinc oxide nanoparticles to bok choy (Brassica chinensis L .) in garden soil. Ecotoxicology and Environmental Safety. 2024;280(May):116519.
40. Xu J, Luo X, Wang Y, Feng Y. Evaluation of zinc oxide nanoparticles on lettuce (Lactuca sativa L.) growth and soil bacterial community. Environmental Science and Pollution Research. 2018;25:6026–35.
41. Liu Y, Li Y, Pan B, Zhang X, Zhang H, Steinberg CEW, et al. Application of low dosage of copper oxide and zinc oxide nanoparticles boosts bacterial and fungal communities in soil. Science of the Total Environment. 2020;143807.
42. Wei X, Cao P, Wang G, Liu Y, Song J, Han J. CuO, ZnO, and γ-Fe2O3 nanoparticles modified the underground biomass and rhizosphere microbial community of Salvia miltiorrhiza (Bge .) after 165-day exposure. Ecotoxicology and Environmental Safety. 2021;217:113222.
43. Sánchez-pérez DM, Marszalek JE, Meza-velázquez JA, Lafuente-rincon DF, Salazar-ramírez MT, Márquez-guerrero SY, et al. Enhancing Nutraceutical Quality and Antioxidant Activity in Chili Pepper (Capsicum annuum L.) Fruit by Foliar Application of Green-Synthesized ZnO Nanoparticles (ZnONPs). Nanomaterials. 2025;15:1440.
44. Uresti-porras J, Fuente MC de la, Benavides-mendoza A, Olivares-Sáenz E, Cabrera RI, Juárez-Maldonado A. Effect of Graft and Nano ZnO on Nutraceutical and Mineral. Plants. 2021;10:2793.
45. Iziy E, Majd A, Vaezi-kakhki MR, Nejadsattari T, Noureini SK. Effects of zinc oxide nanoparticles on enzymatic and nonenzymatic antioxidant content , germination , and biochemical and ultrastructural cell characteristics of Portulaca oleracea L . Acta Societatis Botanicorum Poloniae. 2019;88(4):1–14.
46. Miliauskien J, Brazaitytė A, Sutulienė R, Urbutis M, Tučkutė S. ZnO Nanoparticle Size-Dependent Effects on Swiss Chard Growth and Nutritional Quality. Agriculture. 2022;12:1905.
47. Adnan M, Mahmood F, Zhao Z, Khaliq H. Effect of the foliar application of biogenic-ZnO nanoparticles on physio-chemical analysis of chilli (Capsicum annum L.) in a salt stress environment. Environmental Science: Advances. 2025;(4):306–17.
48. Uresti-porras JG, Fuente MC de la, Benavides-mendoza A, Sandoval- A, Zermeño-gonzalez A, Cabrera RI, et al. Foliar application of zinc oxide nanoparticles and grafting improves the bell pepper (Capsicum annuum L .) productivity grown in NFT system. Notulae Botanicae Horti Agrobotanici Cluj-Napoca. 2021;49(2):12327.
49. Mirakhorli T, Ardebili ZO, Ladan-moghadam A, Danaee E. Bulk and nanoparticles of zinc oxide exerted their beneficial effects by conferring modifications in transcription factors , histone deacetylase , carbon and nitrogen assimilation , antioxidant biomarkers , and. PLOS ONE. 2021;16(9):1–16.
50. Srivastav A, Ganjewala D, Singhal RK, Rajput VD, Minkina T, Voloshina M, et al. Effect of ZnO Nanoparticles on Growth and Biochemical Responses of Wheat and Maize. Plants. 2021;10:2556.
51. Piesik D, Wenda-piesik A, Łyczko J, Lemańczyk G, Bocianowski J, Piesik M. Synergistic use of iron nanofertilizers and biotic elicitors to induce defensive volatile organic compound emissions from Brassica napus. Journal of Plant Protection Research. 2024;64(4):336–46.
52. National Institute of Standards and Technology. NIST Chemistry WebBook [Internet]. Available from: https://webbook.nist.gov
53. Gondor OK, Magda P, Janda T, Szalai G. The role of methyl salicylate in plant growth under stress conditions. Journal of Plant Physiology. 2022;277:153809.
54. Singewar K, Fladung M, Robischon M. Methyl salicylate as a signaling compound that contributes to forest ecosystem stability. Trees. 2021;35:1755–69.
55. Liu B, Kaurilind E, Jiang Y, Niinemets Ü. Methyl salicylate di ff erently a ff ects benzenoid and terpenoid volatile emissions in Betula pendula. Tree Physiology. 2018;00(July):1–13.
56. Liang X, Qian R, Wang D, Liu L, Sun C, Lin X. Lipid-Derived Aldehydes : New Key Mediators of Plant Growth and Stress Responses. Biology. 2022;11:1590.

 doi:10.20944/preprints202601.0199.v1

57. Vincenti S, Mariani M, Alberti J christophe, Jacopini S, Cara VB bronzini D, Berti L, et al. Biocatalytic Synthesis of Natural Green Leaf Volatiles Using the Lipoxygenase Metabolic Pathway. Catalysts. 2019;9:873.
58. Wu J, Zhai Y, Liu G, Bosker T, Vijver MG, Peijnenburg WJGM. Dissolution Dynamics and Accumulation of Ag Nanoparticles in a Microcosm Consisting of a Soil − Lettuce − Rhizosphere Bacterial Community. ACS Sustainable Chemistry and Engineering. 2021;9:16172–81.
59. Wei L, Liu J, Jiang G. Nanoparticle-speci fi c transformations dictate nanoparticle effects associated with plants and implications for nanotechnology use in agriculture. Nature Communications. 2024;15:7389.
60. Maccormack TJ, Clark RJ, Dang MKM, Ma G, Kelly JA, Veinot JGC, et al. Inhibition of enzyme activity by nanomaterials : Potential mechanisms and implications for nanotoxicity testing. Nanotoxicology. 2012;6(5):514–25.
61. Northwick A, Wang Y, Tuga B, Haynes C, Hernandez R, Carlson E. Molecular-Level Characterization of Protein-Nanoparticle Interactions: Orientation, Deformation and Matrix Effects [Internet]. ChemRxiv; 2025 [cited 2025 Dec 19]. Available from: https://chemrxiv.org/engage/chemrxiv/article-details/67746bab81d2151a0284c25d
62. Matsui K. Green leaf volatiles : hydroperoxide lyase pathway of oxylipin metabolism. Current Opinion in plant Biology. 2006;9:274–80.
63. Nel AE, Mädler L, Velegol D, Xia T, Hoek EMV, Somasundaran P, et al. Understanding biophysicochemical interactions at the nano–bio interface. Nature Publishing Group. 2009;8(7):543–57.
64. Dimkpa CO, McLean JE, Latta DE, Britt DW, Johnson WP, Boyanov MI, et al. CuO and ZnO nanoparticles : phytotoxicity , metal speciation , and induction of oxidative stress in sand-grown wheat. Journal of Nanoparticle Research. 2012;14:1125.
65. Park S wook, Kaimoyo E, Kumar D, Mosher S, Klessig D. Methyl Salicylate Is a Critical Mobile Signal for Plant Systemic Acquired Resistance. Science. 2007;318(113).
66. Rico CM, Majumdar S, Duarte-gardea M, Peralta-videa JR, Gardea-torresdey JL. Interaction of Nanoparticles with Edible Plants and Their Possible Implications in the Food Chain. Journal of Agricultural and Food Chemistry. 2011;59:3485–98.
67. Ghosh M, Jana A, Sinha S, Jothiramajayam M, Nag A, Chakraborty A, et al. Effects of ZnO nanoparticles in plants : Cytotoxicity , genotoxicity , deregulation of antioxidant defenses , and cell-cycle arrest. Mutation Research - Genetic Toxicology and Environmental Mutagenesis. 2016;807:25–32.
68. Corso M, Garcia V. tolerance and hyperaccumulation in plants. Metallomics. 2020;
69. Presentato A, Piacenza E, Turner RJ, Zannoni D, Cappelletti M. Processing of Metals and Metalloids by Actinobacteria : Cell Resistance Mechanisms and Synthesis of Metal (loid) -Based Nanostructures. Microorganisms. 2020;8:2027.
70. Schmidt A, Sineriz M, Merten D, Bu G, Kothe E. Heavy metal resistance mechanisms in actinobacteria for survival in AMD contaminated soils. Geochemistry. 2005;65:131–44.
71. Goulsbra AM, Edwards C, Gallagher MP. Surface hygiene monitored using a reporter of fis in Escherichia coli. Journal of applied Microbiology. 2001;91:104–9.
72. Stubbendieck RM, Vargas-bautista C, Straight PD, Romero DF, Beauregard P. Bacterial Communities : Interactions to Scale. Frontiers in Microbiology. 2016;7:1234.